

Dynamic Optimisation of Industrial Sugar Crystallization Process based on a Hybrid (mechanistic+ANN) Model

Vytautas Galvanauskas, Petia Georgieva and Sebastião Feyo de Azevedo¹

Abstract — A model-based optimization of an industrial fed-batch sugar crystallisation process is considered in this paper. The objective is to define the optimal profiles of the manipulated process inputs, the feeding rate of liquor/syrup and the steam supply rate, such that the crystal content and the crystal size distribution (CSD) measures at the end of the batch cycle reach the reference values. A knowledge-based hybrid model is implemented, which combines a partial first principles model reflecting the mass, energy and population balances with an artificial neural network (ANN) to estimate the kinetics parameters - particle growth rate, nucleation rate and the agglomeration kernel. The simulation results demonstrate that the very tight and conflicting end-point objectives are simultaneously feasible in the presence of hard process constraints.

I. INTRODUCTION

Vacuum evaporative crystallisers are widely used in the industrial sugar refining processes. The main goal of these processes is to produce sugar with desired crystal size distribution (CSD) specifications, obeying technological constraints on manipulated inputs and within limited time. The CSD measures - coefficient of variation (CV) and average (in mass) crystal size (MA), and the crystal content, are the main quality criteria of the sugar crystals defined by ICUMSA (International Commission for Uniform Methods of Sugar Analysis).

The main challenge of the batch production is the large batch-to-batch variation of the final CSD (Patience and Rawlings, 2001) and in particular high CV values (above 30%). This lack of process repeatability results in final product recycling and loss increase and is caused by several factors. The most important among them are not proper liquor/syrup feeding and steam supply, leading to high supersaturation, and as a result, sporadically occurring secondary nucleation that increases CV.

V. Galvanauskas is with the Process Control Department, Kaunas University of Technology, Studentų 50, LT-51386 Kaunas, Lithuania (e-mail vytautas.galvanauskas@ktu.lt).

P. Georgieva is with the Department of Electronics and Telecommunications, IEETA, University of Aveiro, 3810-193 Aveiro, Portugal (corresponding author, phone: +351-234-370531; fax: +351-234-370-545; e-mail: petia@det.ua.pt).

S. Feyo de Azevedo is with the Department of Chemical Engineering, Faculty of Engineering, University Porto, Rua Dr. Roberto Frias s/n, 4200-465 Porto, Portugal (e-mail: sfeyo@fe.up.pt).

Due to the highly competitive nature of the today's crystallization industry, model-based optimization becomes increasingly accepted as one of the approaches that can drive the process to its optimal state of profit maximization and cost minimization [Lauret et al., 2000, Nagy and Braatz, 2003]. However, the crystallisation occurs through the complex mechanisms of particle nucleation, subsequent particle growth and agglomeration or aggregation, phenomena that are physically not well understood therefore their reliable modelling is still a challenging task (Fujiwara et al., 2005). Most of the reported crystallizer models neglect the agglomeration effect. For the process in hand this assumption appears to be irrelevant since agglomeration is registered in the process run. Mechanistic models accounting for the three crystallization phenomena usually devolve biased estimation of CV and MA (Georgieva et al., 2003). To overcome this problem a knowledge-based hybrid model (KBHM) was developed which combines a partial mechanistic model reflecting the mass, energy and population balances with an artificial neural network (ANN) for modelling the crystal growth, the nucleation rate and the agglomeration kernel. The model parameters were tuned using industrial process data and applying the Levenberg-Marquart optimisation procedure (Georgieva et al., 2003). This paper is focused on a model-based optimization procedure to determine the optimal profiles of the manipulated process inputs, the feeding rate of liquor/syrup and the steam supply rate, such that the crystal content and the CSD measures at the end of the batch cycle reach the reference values. The main challenge is that the objectives are rather conflicting and difficult to arrive at simultaneously. For example the attempts to reduce CV by means of optimisation of the feeding rate and the steam supply profiles, and simultaneously to control the supersaturation levels, may lead to undesirable growth of MA. Moreover, the hard technological process constraints reduce significantly the space of feasible optimal points and make the optimisation task more complex. However, the application of the stochastic (evolutionary programming) optimization approach (Li and Haussler, 1996) coupled with the ANN-based parameterization of the manipulated inputs, guaranteed better convergence and succeeded to find feasible optimal profiles for all optimization variables (i.e. the manipulated process inputs). The performance of the optimization procedure was evaluated by simulation with rather satisfactory results.

II. PROCESS OPERATION

Sugar crystallisation occurs through the mechanisms of nucleation, growth and agglomeration. The process is characterised by strongly non-linear and non-stationary dynamics and can be divided into several sequential phases.

Charging. During the first phase the pan is partially filled with a juice containing dissolved sucrose (termed liquor). The initial liquid charged in the pan should cover completely the calandria.

Concentration. The next phase is the concentration. The liquor is concentrated by evaporation, under vacuum, until supersaturation reaches a predefined value. At this stage seed crystals are introduced into the pan to induce the production of crystals. This is the beginning of the third (crystallisation) phase.

Crystallisation (main phase). In this phase as evaporation takes place further liquor or water is added to the pan in order to guarantee crystal growth at a controlled supersaturation level and to increase total contents of sugar in the pan. In most cases, due to economical reasons, the liquor is replaced by other juice of lower purity (termed syrup).

Tightening. The fourth phase consists of tightening which is principally controlled by evaporation capacity. The pan is filled with a suspension of sugar crystals in heavy syrup, which is dropped into a storage mixer. At the end of the batch, the final massecuite undergoes centrifugation, where final refined sugar is separated from (mother) liquor that is recycled to the process.

The unit contains 15 sensors for the following properties and operating variables: *i) inside the pan* - massecuite temperatures at three locations; brix of solution; level; massecuite consistency; stirrer current; vacuum pressure and temperature. *ii) feed conditions* - temperature, brix and flow rate of feed liquor and feed syrup. *iii) steam conditions* - temperature, pressure and flow rate of steam.

Brix is the concentration of total dissolved solids (sucrose plus impurities) in the solution. Supersaturation is not a measured variable but can be determined from the available measurements. The feed flow rates of sugar liquor/syrup and the steam supply are considered as process inputs. The crystal contents and the crystal size distribution (CSD) characterise the product quality.

More details about the process can be found elsewhere (Feyo de Azevedo et al., 1994, Georgieva et al., 2003).

III. KNOWLEDGE-BASED HYBRID (MECHANISTIC+ANN) MODEL (KBHM)

Based on the available process measurements a detailed first principles model can be developed. However, it cannot be utilized in the optimization structure because not all of the states are observable. To overcome this problem a knowledge-based hybrid model (KBHM) was obtained where some parts of the model are approximated by an ANN

(Zorzetto et al., 2000). Short description of the model follows below.

A. Mass balance

The mass of water (M_w), impurities (M_i), dissolved sucrose (M_s) and crystals (M_c) are included in the following set of conservation mass balance equations

$$\frac{dM_w}{dt} = F_f \rho_f (1 - B_f) + F_w \rho_w - J_{vap} \quad (1)$$

$$\frac{dM_i}{dt} = F_f \rho_f B_f (1 - Pur_f) \quad (2)$$

$$\frac{dM_s}{dt} = F_f \rho_f B_f Pur_f - J_{cris} \quad (3)$$

$$\frac{dM_c}{dt} = J_{cris} \quad (4)$$

B. Energy balance

The second part of the model is the energy balance

$$\frac{dT_m}{dt} = aJ_{cris} + bF_f + cJ_{vap} + d \quad (5)$$

where J_{vap} is the evaporation rate and a , b , c , d incorporate the enthalpy terms and specific heat capacities derived as functions of physical and thermodynamic properties.

C. Population balance (in volume coordinates)

The kinetic mechanisms of nucleation, crystal growth and particle agglomeration are defined by the population balance. The population balance is expressed by the leading moments of CSD in volume coordinates since the agglomeration phenomenon must obey mass conservation law,

$$\frac{d\tilde{\mu}_0}{dt} = \tilde{B}_0 - \frac{1}{2} \beta' \tilde{\mu}_0^2 \quad (6)$$

$$\frac{d\tilde{\mu}_1}{dt} = G_v \tilde{\mu}_0 \quad (7)$$

$$\frac{d\tilde{\mu}_2}{dt} = 2G_v + \beta' \tilde{\mu}_1^2 \quad (8)$$

$$\frac{d\tilde{\mu}_3}{dt} = 3G_v \tilde{\mu}_2 + 3\beta' \tilde{\mu}_1 \tilde{\mu}_2 \quad (9)$$

where the volume growth rate is determined as

$$G_v = 3k_v^{1/3} \left(\frac{v}{\tilde{\mu}_0} \right)^{2/3} G \quad (10)$$

The kinetic variables (nucleation rate $-B$, linear growth rate $-G$, agglomeration kernel $-\beta$) are replaced by a feed-forward ANN with sigmoid activation functions (4 inputs, 9 nodes in the hidden layer, 3 outputs). The crystallisation rate

is determined as

$$J_{cris} = \rho_c \frac{d\tilde{\mu}_1}{dt} \quad (11)$$

The CSD measures CV and MA are then inferred from the moments (6-9), (see for more details Georgieva et al., 2003).

D. Hybrid ANN training – sensitivity approach

It is well known that the kinetic parameters depend mainly on the temperature (T_m), the supersaturation (S), the purity of the solution (Pur_{sol}) and the volume fraction of crystals (v_c). Therefore, these four variables are considered as networks inputs.

A challenging problem arising by this hybrid network modelling is that it is not possible to apply the usual supervised training procedure. The training of a neural network requires that the network weights are determined in such a way that the error between the network output and the corresponding target output becomes minimal. However, in the hybrid system under consideration, the target outputs are not available since the kinetic parameters are not measured. Hence, a new training procedure is required. A possible scenario is to propagate the network output through some part of the analytical (fixed) model until it arrives to an output for which industrial data are available (see Fig.1).

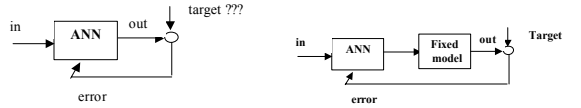


Fig. 1 New supervised ANN training procedure

Among various alternatives, the mass of crystals is considered as the most appropriate to serve as a target output in the hybrid network training (Fig. 2).

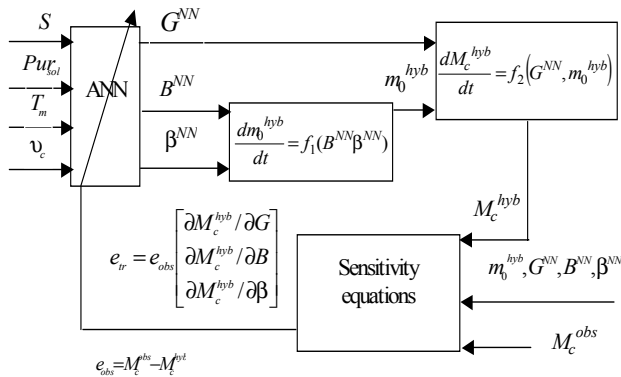


Fig.2: Hybrid training procedure

According to equations (4), (6), (10) and (11), the mass balance of crystals can be rewritten as

$$\frac{dM_c^{hyb}}{dt} = 3(k_v \rho_c)^{1/3} (\tilde{\mu}_0^{hyb})^{1/3} (M_c^{hyb})^{2/3} G^{NN} \quad (12)$$

(12) is incorporated in the hybrid training structure but in order to integrate it $\tilde{\mu}_0$ is also required. Therefore its respective differential equation is involved in the network training stage,

$$\frac{d\tilde{\mu}_0^{hyb}}{dt} = B^{NN} - \frac{1}{2} \beta^{NN} (\tilde{\mu}_0^{hyb})^2 \quad (13)$$

Superscripts hyb and NN are used to point out variables obtained during the hybrid network training. The neural network computes the estimates for the growth rate, the nucleation and the agglomeration kernel. These estimates are propagated through eq. (12-13). The error signal (e_{tr}) for updating the network weights is a function of two terms

$$e_{tr} = e_{obs} [\lambda_G \quad \lambda_B \quad \lambda_\beta]^T \quad (14)$$

It is obtained by multiplication of the observed error (e_{obs})

$$e_{obs} = M_c^{obs} - M_c^{hyb} \quad (15)$$

with the gradient of the hybrid model output with respect to the network outputs

$$\lambda_G = \frac{\partial M_c^{hyb}}{\partial G} \quad (16.1)$$

$$\lambda_B = \frac{\partial M_c^{hyb}}{\partial B} \quad (16.2)$$

$$\lambda_\beta = \frac{\partial M_c^{hyb}}{\partial \beta} \quad (16.3)$$

The gradients (14-16) can be computed through integration of the sensitivity equations

$$\frac{d\lambda_G}{dt} = \frac{\partial f_2}{\partial M_c^{hyb}} \lambda_B + \frac{\partial f_2}{\partial G}, \quad \lambda_G(0) = 0 \quad (17)$$

$$\frac{d\lambda_B}{dt} = \frac{\partial f_2}{\partial M_c^{hyb}} \lambda_B + \frac{\partial f_2}{\partial \tilde{\mu}_0^{hyb}} \left(\frac{\partial \tilde{\mu}_0^{hyb}}{\partial B} \right), \quad \lambda_B(0) = 0 \quad (18)$$

$$\frac{d\lambda_\beta}{dt} = \frac{\partial f_2}{\partial M_c^{hyb}} \lambda_\beta + \frac{\partial f_2}{\partial \tilde{\mu}_0^{hyb}} \frac{\partial \tilde{\mu}_0^{hyb}}{\partial \beta}, \quad \lambda_\beta(0) = 0, \quad (19)$$

where f_2 is the right hand side of (12)

$$f_2 = 3(k_v \rho_c)^{1/3} (\tilde{\mu}_0^{hyb})^{1/3} (M_c^{hyb})^{2/3} G^{NN}.$$

Note, that while λ_c can be straightforward obtained, λ_B and λ_β depend on the gradients of the zero moment with respect to B and β , respectively. In order to determine them the same strategy is used leading to integration of the following sensitivity equations with zero initial conditions

$$\frac{d\chi_B}{dt} = \frac{\partial f_1}{\partial \tilde{\mu}_0} \chi_B + \frac{\partial f_1}{\partial B}, \quad \chi_B(0) = 0 \quad (20)$$

$$\frac{d\chi_\beta}{dt} = \frac{\partial f_1}{\partial \tilde{\mu}_0} \chi_\beta + \frac{\partial f_1}{\partial \beta}, \quad \chi_\beta(0) = 0, \quad (21)$$

where f_1 is the right hand side of (13)

$$f_1 = B^{NN} - \frac{1}{2} \hat{\beta}^{NN} \left(\tilde{\mu}_0^{hyb} \right)^2 \text{ and}$$

$$\chi_B = \frac{\partial \tilde{\mu}_0}{\partial B}, \quad \chi_\beta = \frac{\partial \tilde{\mu}_0}{\partial \beta}.$$

IV. OPTIMISATION PROBLEM

End-point optimization of batch processes, i.e. achievement of the best outcome of a finite end-time process through appropriate manipulation of its input variables is of concern in many practical control applications. For example, in the batch crystallization process the parameters MA, CV and the crystal content are common properties of interest for optimization. The optimization problem can be mathematically formulated as:

$$\max_{u_{\min} \leq u(t) \leq u_{\max}} J_f = \varphi(x(t_f), P), \quad (22)$$

s.t.:

$$\dot{x} = f(x(t), u(t), P), \quad 0 \leq t \leq t_f, \quad x(0) = x_0 \quad (23.1)$$

$$y(t) = h(x(t), P) \quad (23.2)$$

$$g_j(x) = 0, \quad j = 1, 2, \dots, p \quad (24.1)$$

$$v_j(x) \leq 0, \quad j = 1, 2, \dots, l \quad (24.2)$$

where (22) is the performance index, (23) is the process model, function f is the state-space description, function h is the relationship between the output and the state, P is the parameter vector and t_f is the final batch time.

$x(t) \in R^n$, $u(t) \in R^m$ and $y(t) \in R^p$ are the state, the manipulated input, also known as the control decision variable, and the control output vectors, respectively. The manipulated inputs, the state and the control outputs are subject to the following constraints, $x(t) \in X$, $u(t) \in Z$, $y(t) \in Y$ in which X , Z and Y are convex and closed subsets of R^n , R^m and R^p . g_j and

v_j are the equality and inequality constraints with p and l dimensions respectively.

We apply here the practical approach of reformulating the optimization problem (22) and the process constraints (24) in an unified structure through the use of a penalty function in the performance index. It is a simple and intuitive way to include the constraints in the optimization procedure as an extra term in the performance function

$$\max_{u_{\min} \leq u(t) \leq u_{\max}} J = \alpha_1 J_f + \alpha_2 \sum_{j=1}^p (g_j)^2 - \alpha_3 \sum_{j=1}^l [\max(0, v_j)]^2 \quad (25)$$

where g_j and v_j are the constraints defined in (24) and α_i , $i = 1, 2, 3$ are the weighting factors.

V. OPTIMIZATION PROCEDURE

Process performance index

The crystallizer performance index J_f (related to the final time objectives) has several components. The first objective is to achieve crystals with a desired final size, which is quantified by the quality variable MA. It is practically more relevant instead of defining a fixed end-setpoint for MA to choose a tight zone around the desired value. For the process considered these are $MA_{\min} = 0.55$ and $MA_{\max} = 0.60$. Therefore

$$MA_{\min} \leq MA(t_f) \leq MA_{\max} \quad (26)$$

The second objective is reducing the quality variable CV as much as possible. But in practice CV less than a predefined limit is enough for good performance. Then

$$CV(t_f) \leq CV_{\max}, \text{ with } CV_{\max} = 30\% \quad (27)$$

To guarantee sufficient efficiency of the production, the crystals should occupy a certain minimum volume of the pan. This objective is quantified by the crystal content (wc)

$$wc_{\min} \leq wc(t_f), \text{ with } wc_{\min} = 50\% \quad (28)$$

The main process constraints are related to the supersaturation and the volume of the pan during the batch. In case the supersaturation is below a minimum value, the crystals start dissolving and if the supersaturation is above a maximum value, undesired secondary nucleation takes place. Therefore

$$S_{\min} \leq S(t) \leq S_{\max} \quad (29)$$

where for the process in hand reasonable limiting values are $S_{\min} = 1.02$, $S_{\max} = 1.25$. The total volume is limited by the physical dimensions of the pan. Hence

$$V(t) \leq V_{\max}, \text{ with } V_{\max} = 35$$

(30) approaching the optimum (Pham, 1998).

The decision variables of the optimisation (the process inputs) are the feeding rate (F_f) and the steam supply rate (F_s). The optimal switching time between liquor and syrup supply t_{syr} was also considered as an optimisation parameter. Due to technological limits of the process equipment, F_f and F_s are up and down limited which is considered as a hard constrain of the optimisation procedure. The values of steam and feed temperatures, purities and brix of the syrup and liquor, vacuum pressure are averaged based on the available industrial data and during the simulations are kept constant. The process time is fixed to 90min. The averaged values of the operational parameters and the input constraints are summarised in Table 1.

Taking into account (26-30), the general multi-objective optimization performance index in (22) has the following particular structure:

$$\begin{aligned}
 J = & -\alpha_1 [\max(0, AM_{\min} - AM(t_f))]^2 - \\
 & \alpha_2 [\max(0, AM(t_f) - AM_{\max})]^2 - \\
 & \alpha_3 [\max(0, CV(t_f) - CV_{\max})]^2 - \\
 & \alpha_4 [\max(0, wc_{\min} - wc(t_f))]^2 - \\
 & \alpha_5 [\max(0, S_{\min} - S(t))]^2 - \\
 & \alpha_6 [\max(0, S(t) - S_{\max})]^2 - \\
 & \alpha_7 [\max(0, V(t) - V_{\max})]^2.
 \end{aligned}$$

and the optimisation problem (22) can be stated as follows:

$$\max_{\{F_{\min} \leq F_f(t) \leq F_{\max}; F_{s \min} \leq F_s(t) \leq F_{s \max}; t_{syr}\}} J \quad (32)$$

subject to: equations (1-11)

Several methods can tackle the optimisation problem (32). The derivative based deterministic methods are rather sensitive to the model initial conditions and do not guarantee a global optimum but they are faster than the stochastic methods and are usually more appropriate to on-line optimisation. Since the aim was to find *off-line* the optimal profiles of the manipulated inputs that lead to maximisation of the process performance index at the end of the process, the stochastic approach appears to be more efficient solution. In particular, the evolutionary programming was considered as the method with less sensitivity to the scaling of the multidimensional performance index and good convergence

TABLE 1. AVERAGED PROCESS PARAMETERS AND INPUT CONSTRAINTS

Parameter	Value
Pur_{liq}	0.999
Pur_{syr}	0.955
B_{liq}	0.72
B_{syr}	0.765
T_f	65 [°C]
T_s	137 [°C]
P_s	2.1 [bar]
F_{smin}	1.1 [kg/s]
F_{smax}	2.1 [kg/s]
F_{fmin}	0.0 [m ³ /s]
F_{fmax}	0.0275 [m ³ /s]

To relax the numerical procedure the optimization variables are usually parameterised as piece wise constant, linear or polynomial functions. However, it means less freedom in determining their final values and leads to suboptimal profiles. To deal with this problem we express each optimization variable as a general nonlinear time function (Galvanuskas et al., 1998)

$$F_i(t) = f_i(a_1, a_2, \dots, a_k, t), \quad i = \{s, f\}, \quad (33)$$

where t is the time and a_1, a_2, \dots, a_k are parameters to determine. Then employ an ANN with a single layer and radial-basis functions (RBF) as the activation units to approximate (33)

$$f_i(a_1, a_2, \dots, a_k, t) = \sum_{j=1}^k w_j \Phi_j, \quad i = \{s, f\} \quad (34)$$

where w_j are the NN weights and Φ_j are Gaussian functions, determining bell shaped relationships:

$$\Phi_j(t) = \exp\left(-\frac{(t-c_j)^2}{\rho_j^2}\right). \quad (35)$$

Note that c_j is the time grid for RBF and ρ_j define the shape of RBF. In the analysed case c_j is equal to equidistantly divided time grid with $k=8$ and $\rho_j=400$.

The iterative optimisation procedure is summarized in Fig. 3. The following steps can be distinguished :

1) Assigning initial values of the process states and all parameters subject to optimization - w_j and the switching time between liquor and syrup t_{syr} .

2) Computation of the manipulated inputs (33) by solving (35) and (34) for each variable.

3) Computation of the nucleation rate (\tilde{B}_0), the growth rate (G) and the agglomeration kernel (β^*) by the trained ANN. The ANN outputs are calculated at each integration step, and the necessary input values S, T_m, v_c, Pur_{sol} are

supplied from the current state variables and derived quantities, calculated in the previous integration time instant.

4) The system of differential equations (1-11) is then solved and the CSD measures CV and MA are derived.

5) The current values of the performance index components are compared with the reference values (26-30) and the overall performance index (31) is computed.

6) The performance index is evaluated and the evolutionary programming technique generates a new set of w_j and t_{syr} . The procedure repeats starting from the step 2.

7) If no improvements of the performance index (31) is achieved within a predefined iteration number or the relative iteration-to-iteration change is insignificant the procedure is stopped and the final optimal profiles are generated.

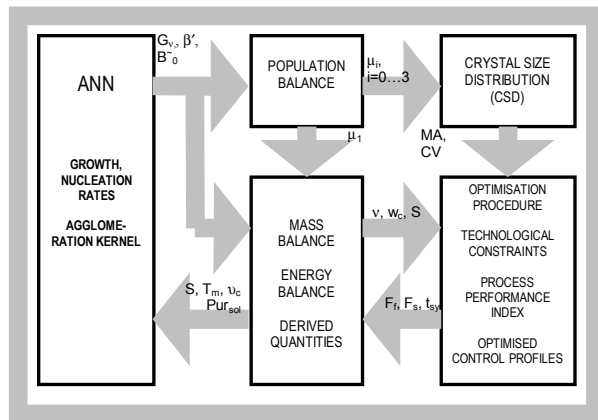


Fig.3. Structural scheme of the optimisation procedure

VI. RESULTS AND DISCUSSION

The simulation results are summarised in Figs. 4-7. The optimal profiles of the steam supply rate and the feeding rate of liquor/syrup with the respective switching time between liquor and syrup are depicted in Fig. 4. Based on these optimal input profiles (determined by the optimization procedure), the optimal trajectories for the process outputs are estimated by the model. The optimal profiles of the supersaturation (Fig.5a), the brix (Fig.5b) and the masecuite temperature (Fig.5c) can be used then as setpoints in a feedback control framework.

Fig. 6 shows the main process quality variables along the batch. Though the PSD objectives are related only with the final values, the smooth behaviour of MA (Fig.6a) and CV (Fig.6b) contribute to a higher process internal performance. Note that the MA final value (0.6mm) is within the margins defined by (26) and the $CV=28.2\%$ is also less than the upper limit defined by (27). Moreover it is much less than the average values of CV (37%-39%) obtained in the real plant production (Georgieva et al., 2003). The third objective, quantified by (28), is also satisfied. The crystal content (Fig.7a) at the process end was 57% of the total volume (Fig. 7b). The main process constrains related to the supersaturation and the total volume (29-30) remain within the predefined limits. $V(t_f)=29m^3$ corresponds to

approximately 90% utilisation of the working volume which is considered as a reasonable compromise between productivity and safetiness.

Simulations with the off-line model-based optimisation strategy discussed in this paper demonstrate that the very tight and conflicting end-point objectives are simultaneously feasible in the presence of hard process constrains. Moreover it led to a significant improvement in the CV measure of the industrial sugar crystallisation process as compared to statistically averaged value of CV achieved by the industrial data.

For successful implementation of the optimised control strategy in practice, accurate tracking of the optimised profiles is required. However, the presence of inevitable disturbances occurring in the process variables like brix, purity and temperature of feeding solution, vacuum pressure or steam temperature can make the manipulated inputs not optimal any more. A closed loop control is usually the most effective solution where an on-line input correction is performed based on the current measurements. These issues are not treated in this paper but work on them is now in progress (Georgieva and Fejo de Azevedo, 2006).

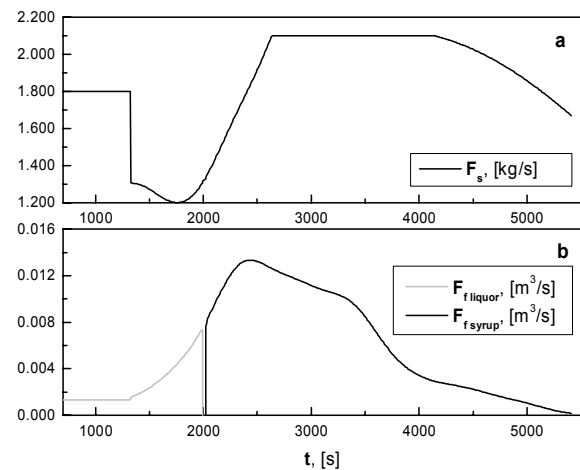


Fig.4. Optimised steam supply (a) and feeding rate (b) profiles, and the optimal switching time.

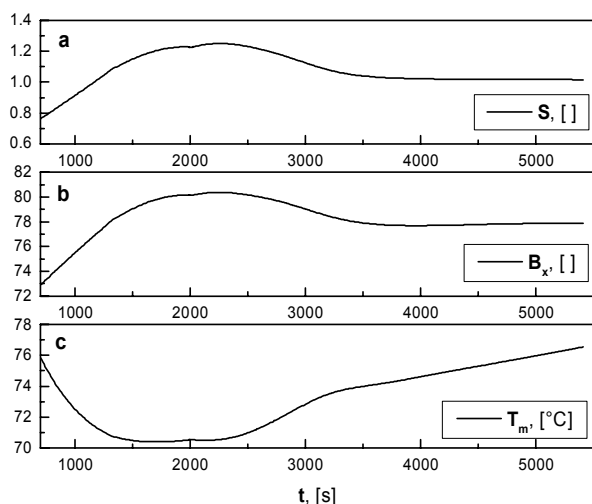


Fig. 5. Supersaturation (a), brix (b) and temperature (c) profiles resulting from the optimised control strategy.

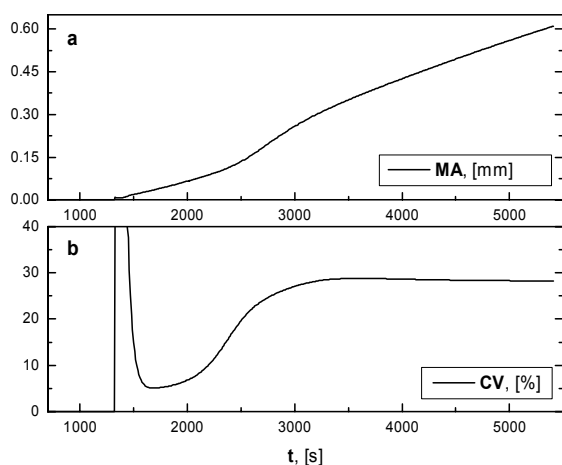


Fig. 6. Average (in mass) crystal size MA (a) and coefficient of variation CV (b) resulting from the optimised control strategy.

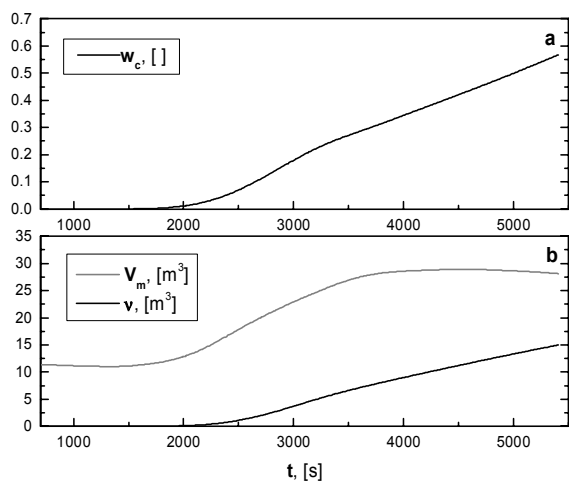


Fig. 7. Crystal content (a), the total (massecuite) volume and the crystal volume (b) resulting from the optimised control strategy.

NOMENCLATURE

B_0	Nucleation rate, [$1/m^3s$]
Bx	Brix (mass fraction of dissolved solids)
CV	Coefficient of variation, [%]
F_f	Feed flow rate, [m^3/s]
F_s	Steam flow rate, [kg/s]
G	Linear growth rate, [m/s]
G_v	Overall crystal volume growth rate, [m^3/s]
J	Process performance index
k_v	Volume shape factor
μ_j	j-moment of number-volume distribution function
M	Mass, [kg]
MA	Averaged (in mass) crystal size, [m]
Pur	Purity (mass fraction of sucrose in the dissolved solids)
S	Supersaturation
t	Time, [s]
T	Temperature, [°C]
V	Volume, [m^3]
w_c	Crystal content
β'	Agglomeration kernel at any time for vessel volume, [$1/s$]
v	Crystal volume, [m^3]
ρ	Density, [kg/m^3], RBF parameter
v_c	Volume fraction of crystals
Subscripts	
c	crystals
$cris$	crystallisation
f	feed
i	impurities
liq/syr	liquor / syrup
m	massecuite
sol	solution
vac	vacuum
vap	evaporation
w	water
Superscripts	
\sim	based on total vessel volume, ($\tilde{x} = xV_m$)

ACKNOWLEDGMENT

This work was pursued in the framework of EC RTN Project BatchPro HPRN-CT-2000-0039. It was further financed by the Portuguese Foundation for Science and Technology within the activity of the Research Unit IEETA-Aveiro, which is gratefully acknowledged.

REFERENCES

- [1] Fujiwara, M. Z. K. Nagy, J. W. Chew, and R. D. Braatz First-principles and direct design approaches for the control of

- pharmaceutical crystallization. *J. of Process Control*, 15:493-504, 2005 (invited).
- [2] Galvanuskas, V., Simutis, R., Volk, N. and Lübbert, A., 1998, Model Based Design of a Biochemical Cultivation Process. *Bioprocess and Biosystems Engineering*, 18(3):227-234.
 - [3] Georgieva P., Meireles, M. J. and Feyo de Azevedo, S., 2003, KBHM of fed-batch sugar crystallization when accounting for nucleation, growth and agglomeration phenomena. *Chem Eng Sci*, 58:3699-3711.
 - [4] L.F.M. Zorzetto, R. Maciel Filho and M. R. Wolf-Maciel, "Process modelling development through artificial neural networks and hybrid models", *Computers and Chemical Engineering*, 24, 1355-1360, 2000.
 - [5] Li, Y. and Haussler A., 1996, Artificial evolution of neural networks and its application to feedback control. *Artificial Intelligence in Engineering*, 10:143-152.
 - [6] Nagy Z. K. and R. D. Braatz,. Robust nonlinear model predictive control of batch processes. *AIChE J.*, 49:1776-1786, 2003.
 - [7] P. Georgieva and S. Feyo de Azevedo, Application of feed forward neural networks in modeling and closed loop control of a fed-batch crystallization process, International Conference on Computer Science, Vienna, Austria, 29-31 March 2006, *Transactions on Engineering, Computing and Technology*, ISSN 1305-5313, p. 65-70.
 - [8] P. Lauret, H. Boyer, and J.C. Gatina, "Hybrid modelling of a sugar boiling process", *Control Engineering Practice*, 8, 299-310, 2000.
 - [9] Patience, D. B. and J. B. Rawlings. Particle-shape monitoring and control in crystallization processes. *AIChE J.*, 47(9):2125–2130, Sept. 2001.
 - [10] Pham, Q.T., 1998, Dynamic Optimization of Chemical Engineering Processes by an Evolutionary Method. *Computers and Chem. Eng.*, 22:1089-1097.